Analysis of Contact Lengths of Strands with Cu Sleeves in CICC Joints*)

Shinobu NAKAZAWA, Daichi ARAI, Toshiya MORIMURA, Daisuke MIYAGI, Makoto TSUDA, Takataro HAMAJIMA, Tsuyoshi YAGAI[1], Yoshihiko NUNOYA[2], Norikiyo KOIZUMI[2], Kazuya TAKAHATA[3] and Tetsuhiro OBANA[3]

Tohoku University, 6-6-05 Aoba Aramaki, Aoba-ku, Sendai, Miyagi 980-8579, Japan
[1]*Sophia University, 7-1 Kioicho, Chiyoda-ku, Tokyo 102-8554, Japan*
[2]*Japan Atomic Energy Agency, 801-1 Mukoyama, Naka., Ibaraki 311-0193, Japan*
[3]*National Institute for Fusion Science, 322-6 Oroshi-cho, Toki, Gifu 509-5292, Japan*

(Received 8 December 2011 / Accepted 19 July 2012)

Cable-in-Conduit-Conductor (CICC) is used for the international thermonuclear fusion experimental reactor (ITER) toroidal field (TF) coils. But the critical current of the CICC is measured lower than expected one. This is partly explained by unbalanced current distribution caused by inhomogeneous contact resistances between strands and copper sleeves at joints. Current density in some strands reaches the critical under unbalanced current, and the quench is occurred under smaller transport current than expected one. In order to investigate the contact resistances, we measure the three-dimensional positions of all strands inside the CICC for Large Helical Device (LHD) poloidal field (PF) outer vertical (OV) coil, and evaluate contact parameters such as number and lengths of strands which contact with a copper sleeve. Then, we simulate the strand positions in the CICC using the numerical code which we developed, and compare the contact parameters which evaluated from the measured strand positions and the simulated ones. It is found that the both results are in good agreement, and the developed numerical model is useful for evaluation of the contact parameters. We apply the code to various CIC conductor joints to obtain optimal joint parameters.

Keywords: cable-in-conduit conductor, contact length, joint, twist pitch

DOI: 10.1585/pfr.7.2403143

1. Introduction

A Cable-in-Conduit-Conductor (CICC) has large mechanical strength and high current density, generally used for large scale superconducting coils such as fusion magnet. The CICC consists of a conduit (jacket) and a twisted cable surrounded by a thin stainless tape, which is assembled with superconducting strands in multiple-stage. Since the coils are assembled with several double pancakes, both terminals of the two coils are jointed and electrically connected in series. In the international thermonuclear fusion experimental reactor (ITER) toroidal field (TF) coils, two cables are set into copper sleeve at the joint. And the current flows through the copper sleeve from one cable to the other one. In order to obtain a uniform contact resistance distribution between the copper sleeve and strands, all strands should appear on the cable surface and have uniform contact with the copper sleeve. However in the real CICC, all strands do not contact uniformly with the copper sleeve, and the contact resistance distribution becomes inhomogeneous.

In some experiments, it is observed that the critical current of the CICC is lower than the expected one. It is partly explained by the inhomogeneous contact resistance between the strands and the copper sleeve at the joint section. This mainly induces an inhomogeneous current distribution, and some strands reach the critical current earlier than the others [1–4].

It is important to investigate the contact resistance distribution at the joint of the CICC. In a first attempt, we identified the three-dimensional positions of all 486 strands of the CICC for Large Helical Device (LHD) Poloidal field (PF) coils [5] and evaluated contact lengths between strands and the copper sleeve [1] for the same lap joint construction as the ITER TF coils. It was proven by this method that the distribution of the contact lengths was not uniform at the joint section.

In this paper, we firstly analyze all strand positions inside the CICC of LHD inner vertical (IV), inner shaping (IS) and outer vertical (OV) coil which have different twist pitches. Secondly, we evaluate the contact lengths between all strands and the copper sleeve. Finally, we search the optimal contact resistance distribution, where all strands appear on the cable surface and contact to the copper sleeve.

author's e-mail: tsuda@ecei.tohoku.ac.jp

*) This article is based on the presentation at the 21st International Toki Conference (ITC21).

2. Evaluation Method of Strand Paths

2.1 Simulation of strand paths

In order to evaluate the contact lengths between the strands and the copper sleeve, we develop a numerical code that analyzes all strand paths in the CICC. We assume following two assumptions.

1) The same order sub-cables have equal area on the cable cross section.
2) According to the cable manufacturing process, the (n-1)-th sub-cables rotate around the centroid of the n-th sub-cable at the cross section through a die to form the n-th sub-cable.

Figure 1 shows schematic view of analyzing strands locations. At first, we draw a cross section of the 5th cable and calculate the boundary line of the 4th order sub-cables. In the case of the calculation of the boundary line of the 4th order sub-cables, we draw an arbitrary reference line from the centroid of the 5th sub-cable, dividing the 5th sub-cable area into 4th sub-cables with equal area as shown in Fig. 1. We carry on this process. Finally, we obtain the centroids in the 1st sub-cable area, which correspond to the centroids of all strands as shown in Fig. 1.

At the arbitrary cross section, the (n-1)-th sub-cables rotate around the centroid of the n-th sub-cable. Here, we take z-axis as longitudinal direction, being parallel to vertical direction to the cable cross section as shown in Fig. 1. And θ_n is phase angle of n-th sub-cable reference line at the arbitrary coordinate z. θ_n increases according to n-th twist pitch along the z-axis and is described as follows,

$$\theta_n = \theta_{n0} + \frac{2\pi}{P_n} z, \tag{1}$$

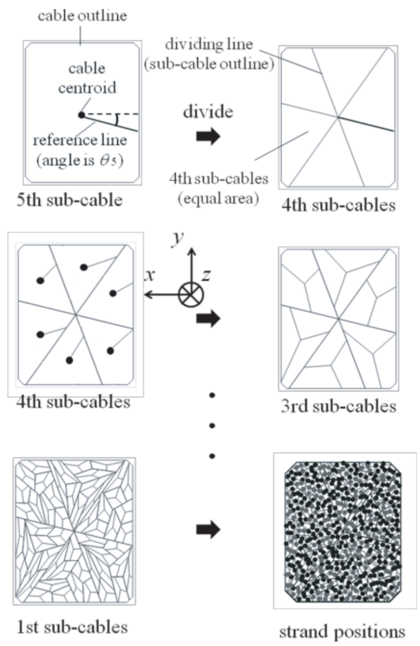

Fig. 1 Schematic view of division and strand locations in cable cross-section.

where, θ_n is an initial phase angle of the reference line at z = 0, P_n is the twist pitch of the n-th sub-cable. In this way, we can analyze all strand positions in the CICC along the longitudinal z-direction.

2.2 Evaluation of contact length

The joint of the CICC ITER TF coils configuration is schematically shown in Fig. 2. At the joint of the ITER TF coils, the jacket of the CIC and the thin stainless tape are unwrapped. Then, the coated chromium on the strand surface is removed, and the surface of the cable is pre-soldered. The soldered cable is set into a copper sleeve whose length is the final cable twist pitch of the cable.

We evaluate the contact lengths between the strands and the copper sleeve inside the joint using the analyzed strand positions. When the surface soldered cable is compacted into the copper sleeve at the joint, the strands inside the cable will be pushed into the inner area, while the strands on the cable surface will have contact to the copper sleeve. It is assumed that strands outside the outline of the compacted cable at the joint, should contact with the copper sleeve as shown in Fig. 3. The strands which contact with a copper sleeve are drawn by black dots. The total

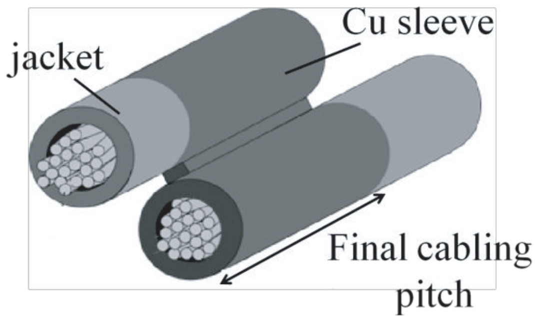

Fig. 2 Schematic view of joint configuration for ITER TF coils.

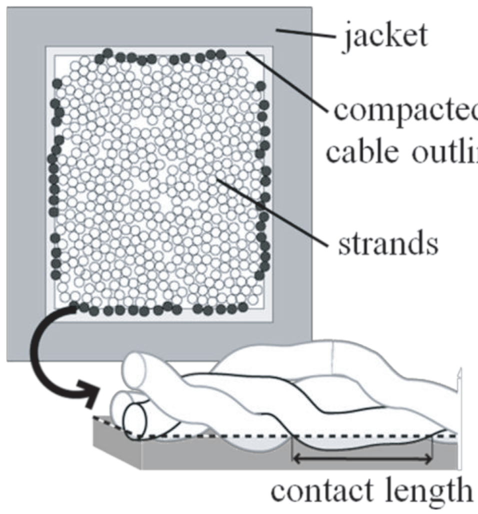

Fig. 3 Schematic view of the contacting strands with Cu sleeves in the cable cross-section.

contact length of the strand is defined as the summation of the contacting lengths of the strand appearing on the compacted cable surface along the longitudinal z-direction.

3. Results and Discussion

3.1 Specification of CICC

Table 1 show the main parameters of the CICC for the LHD OV and IV, IS coils. The cable is composed of NbTi strands and twisted in 5 stages. The cable for IV, IS coils have shorter twist pitch than that for OV coils, while the final twist pitches of both cables are equal. The both strand diameters, conductor sizes and joint diameters are little bit different. The length of joint is assumed to be the final twist pitch.

3.2 Evaluation of contact length

Firstly, we estimate the strand positions of each CICC using our numerical code. The cross section of inner conduit is rectangle, but strands in actual OV conductor have not located in the rectangular corner due to the wrapping of 5th cable. Therefore, the outer shape of 5th cable has octagon-shaped cross-section which is the shape that triangle with height and base are 2 mm is taken away from corner of rectangular inner conduit, as shown in Fig. 1.

Secondly, we estimate the contact length between copper sleeve and strands using the strand paths we measured [1]. And we consider the result as "measured contact length". The histograms of the contact lengths for OV cables estimated from the measured strand paths and the calculated ones are shown in Fig. 4. The both contact parameters are also listed in Table 2. It is found that the both histograms are in good agreement, and the developed numerical code is able to evaluate the contact lengths of the strands.

Finally, we evaluate the contact parameters of strands for OV and IV, IS cables. The histograms of the computed contact lengths are shown in Fig. 5. The calculated contact parameters are also listed in Table 3. The both cables have a lot of strands whose contact lengths are zero. The number of contact strands of IV, IS cable is larger than that of OV cable, and the standard deviation of IV, IS is shorter than that of OV. This may be considered that twist pitch of IV, IS cable is shorter.

3.3 Optimal strand positions

In order to improve the contact length distribution, we simulate many cases about the combination of twist pitches.

Firstly, we analyze the strand paths by varying the twist pitches of 1-st to 4-th sub-cable at 10 mm intervals in the ranges as listed in Table 4. And 5-th twist pitch always keeps the original one. Secondly, we evaluate the contact length between the strands and copper sleeve using the analyzed strands paths each twist pitches. Finally, we calculate the number of non-contact strand and standard deviation of contact length, and determine that the twist

Table 1 Specifications of CIC Conductors.

	IV, IS	OV
Strand diameter	0.76	0.89
Conductor size	17.0×21.6 mm	20.5×24.8 mm
Joint	15.4×20.8 mm	18.7×23.0 mm
Joint length	400 mm	
Void fraction	38 %	
Cable layout	3×3×3×3×6 = 486	
Twist pitch sequence 1st/2nd/3rd/4th/5th	60/100/150/220/ 400 mm	70/120/170/250/ 400 mm

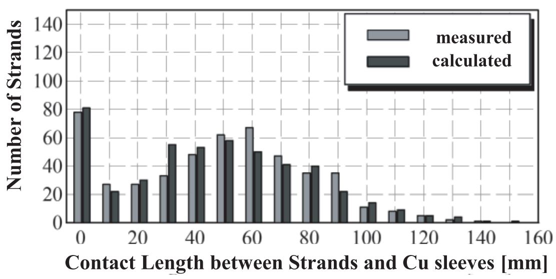

Fig. 4 Comparison of contact lengths for OV cables which evaluated from measured strand paths and the simulated ones at joint part 400 mm in length.

Table 2 Result of contact length measured and calculated (OV).

Parameters	Measured	Calculated
Non-contact strand number	71	69
Average contact length	45.98 mm	47.36 mm
Longest contact length	145.72 mm	142.72 mm
Standard deviation	32.12 mm	31.8 mm

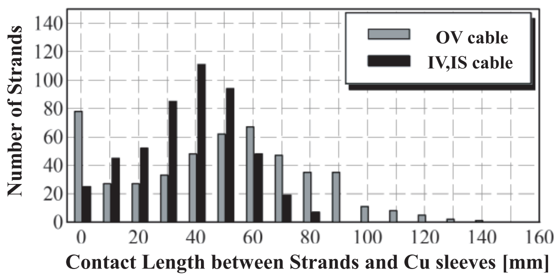

Fig. 5 Comparison of contact lengths of OV with IV, IS cables ones at joint part 400 mm in length.

Table 3 Result of contact length of CICC for LHD.

	IV, IS	OV
Non-contact strand number	20	71
Average contact length	36.6 mm	45.98 mm
Longest contact length	84.1 mm	145.72 mm
Standard deviation	18.0 mm	32.12 mm

Table 4 Search ranges of twist pitches.

Range [mm]		Maximum
5th twist pitch	400	
4th twist pitch	180	380
3rd twist pitch	120	360
2nd twist pitch	80	180
1st twist pitch	40	70

Table 5 Result of contact length both of the original pitches and optimized ones (IV, IS).

	Original	Optimized
Twist pitch sequence 1st/2nd/3rd/4th/5th	60/100/150/ 220/400 mm	40/80/130/ 220/400 mm
Non-contact strand number	20	0
Average contact length	36.6 mm	35.8 mm
Longest contact length	84.1 mm	100.6 mm
Shortest contact length	0	2.0 mm
Standard deviation of contact length	18.0 mm	13.7 mm

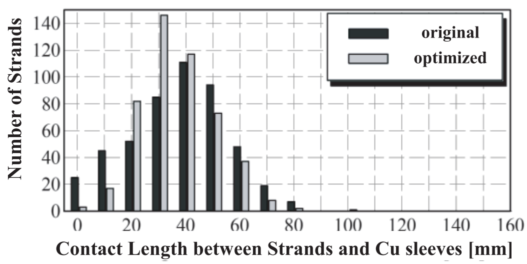

Fig. 6 Histogram of contact length of IV, IS cable both original and optimized pitches at 400 mm joint length.

pitches are optimized if the number of non-contact strand is zero and standard deviation is smallest.

In this way, we obtain the optimized twist pitches of '40/80/130/220/400 mm', from the 1st sub-cable to the 5th cable, respectively. The histogram of the optimized contact lengths is shown in Fig. 6 and the optimized contact parameters are listed in Table 5. All strands appear on the cable surface and have contact with the copper sleeve. And moreover the standard deviation of the contact lengths is small compared to that of the original twist pitches.

It is expected that this pattern is useful for joints of the ITER TF coils. But in fact, the performance of Nb_3Sn strands, which are used for CICC for ITER TF coils, drops by strand being bended. The numerical code we developed must be used in mind bending strain of Nb_3Sn strands. Because the total performance of CICC for ITER TF coils can drop Nb_3Sn strands being bended though the inhomogeneous contact resistance between the strands and the copper sleeve at the joint section is improved changing twist pitches.

4. Conclusion

We evaluate the contact lengths between the strands and the copper sleeve by using the analyzed strand positions. It is found that there are many strands not contacting with the copper sleeve. Moreover, many strands contact to copper sleeve at the cable which has short twist pitches. In order to improve the contact situation, we analyze all strand positions by varying all twist pitches of all sub-cable stages. In the result, we obtain the optimal twist pitches, which all strands appear on the cable surface and contact the copper sleeve with a smaller standard deviation than that of the original ones. Therefore, it is expected to obtain a less imbalanced current distribution.

[1] S. Nakazawa, S. Teshima, D. Arai, D. Miyagi, M. Tsuda, T. Hamajima, T. Yagai, Y. Nunoya, N. Koizumi, K. Takahata and T. Obana, "Analysis of Length Distribution of Superconducting Strands with Copper Sleeves at Cable-in-conduit Conductor Joints," TEIONKOUGAKU (in Japanese) **46**, 8 (2011) to be published in Cryogenics.

[2] N. Koizumi, K. Matsui and K. Okuno, Cryogenics **50**, 129 (2010).

[3] E.P.A. van Lanen and A. Nijhuis, Cryogenics **50**, 139 (2010).

[4] F. Bellina and P. Bruzzone, IEEE Trans. Appl. Supercond. **18**, No.2, 1092 (2008).

[5] T. Yagai, Y. Shibata, J. Ohmura, M. Tsuda, T. Hamajima, Y. Nunoya, K. Okuno and K. Takahata, IEEE Trans. Appl. Supercond. **19**, No.2, 2387 (2009).